Preform Design in Metal Forming

S. Badrinarayanan, A. Constantinescu * and N. Zabaras
Sibley School of Mechanical and Aerospace Engineering, Cornell University, Ithaca, NY 14853

ABSTRACT: A major objective in metal forming is the determination of the initial shape of the workpiece (preform) and of the process parameters (e.g. the die shape) that lead to a final product with desired geometry and material properties. The solutions to these inverse problems are usually obtained by trial and error methods using the results of direct analysis for each set of preforms and process parameters. Sensitivity analysis facilitates a rigorous mathematical formulation and solution of preform and process design problems. In an earlier work (Badrinarayanan and Zabaras 1995), a sensitivity analysis was presented for determining the optimal shape of extrusion dies that leads to a desired material state in the final product. In this work, we concentrate on the formulation and the finite element solution of preform design problems. In particular, the objective is to design the initial shape of the workpiece that when it deforms under the action of a given die, results in a final product with a desired material state and geometry. Shape sensitivities are defined in a rigorous sense and the entire analysis is performed in a fully infinite dimensional setting. An example problem is solved in axisymmetric disk forging where the preform is designed such that, after forging with a flat die, a product with a minimum barreling effect is achieved.

1 INTRODUCTION

In a given forming process, the material state and geometry of the final product depend on several process parameters (loading conditions, geometry of the die surfaces, die lubrication conditions, geometry of the initial workpiece and other). Considering a fixed amount of deformation induced in a given forming process, one may want to control the process parameters in such a way that a final product with a desired material state and geometry can be achieved.

The design of forming processes can also be considered as the design of the initial workpiece and of the subsequent shapes at each of the forming stages known as *preforms*. A systematic study of these problems was done by Kobayashi and colleagues (see Kobayashi et. al. 1989 for a complete set of references). They introduced the so called 'backward tracing technique' and "traced backward the loading path in the actual forming process from a given final configuration."

The preform design and the die design problems can be formulated under a rigorous mathematical basis by posing them as optimization problems (Zabaras and Badrinarayanan 1993). The objective function for these optimization problems can be defined as an appropriate measure of the error between the desired final state and the numerically calculated state for a given set of design variables. In order to solve such optimization problems, one usually employs a sequential search method starting from a reference solution. Sensitivity analysis is a method widely used to evaluate the gradients of the objective functions. Sensitivities can be calculated either by employing finite differences, direct differentiation techniques or the adjoint variable method (Tortorelli and Michaleris 1994, Vidal and Haber 1993, Lee and Arora 1993). Since the problems under consideration are highly non-linear and history dependent, the direct differentiation method (DDM) is the most suitable one. In DDM, the governing equations are directly differentiated to obtain a set of field equations for the sensitivity fields.

We had earlier developed the DDM for die design problems (Badrinarayanan and Zabaras 1995). In these problems, the initial configuration of the body remains the same while the shape of the die surface changes. However, in the case of preform design, the initial configuration of the workpiece is the main unknown of the problem. To define the sensitivity of the deformation gradient, a reference

*on leave from *Laboratoire de Mécanique des Solides* (CNRS URA 317) Ecole Polytechnique, 91128 Palaise au cedex, France

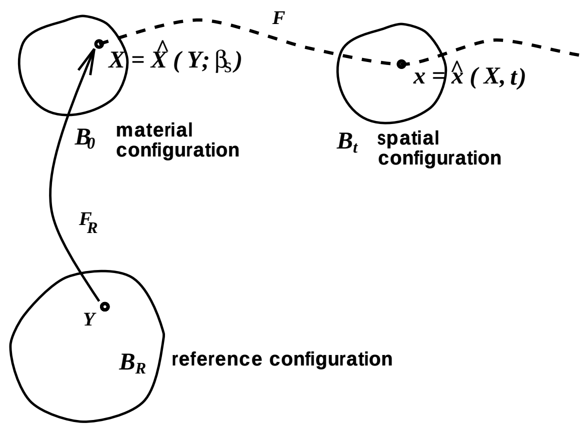

Figure 1: The reference, material and spatial configurations

configuration is introduced that is independent of the shape of the preform. A sufficiently smooth family of mappings are defined from the reference configuration to the preform. Optimization will be performed on this family of mappings.

The equilibrium equation is directly differentiated to obtain the corresponding equation for the sensitivity displacement field. A weak form of this equation is defined and solved using the FEM with exactly the same spatial and temporal discretizations as for the direct deformation analysis. In traditional literature for solving similar problems, the sensitivity problem is formulated on the discretized equations. In such formulations, the evaluation of the "force terms" and the application of the boundary conditions become extremely difficult. However, in the method proposed here, the boundary conditions and the "force terms" for the sensitivity problem, take a form similar to that of the direct analysis.

In the following, the definition of the sensitivity problem will be presented together with its weak form. In order to demonstrate the effectiveness of the present method, an example problem is solved to design the preform shape that when compressed with a flat die, results in a final product with minimum barreling effects.

2 THE CONFIGURATIONS

We consider the workpiece in the following configurations (see figure (1)):

- the *reference* configuration: $\boldsymbol{B}_R$.
  $\boldsymbol{Y}$ will denote an arbitrary point in this configuration. The points of this configuration do not have any material significance.

- the *material* configuration: $\boldsymbol{B}_0$, at time $t = 0$.
  This configuration represents the initial state of the material that undergoes the deformation process, and the material points of this configuration will be denoted by $\boldsymbol{X}$. The configuration $\boldsymbol{B}_0$ is completely described by a sufficiently smooth *reference map* of the form:

$$\boldsymbol{X} = \hat{\boldsymbol{X}}\left(\boldsymbol{Y};\beta_s\right) \tag{1}$$

  where in general β_s are smooth functions that define the whole or parts of $\partial\boldsymbol{B}_0$. The above geometric map does not have a physical meaning and it is introduced only for the purpose of differentiating Lagrangian fields defined in the $\boldsymbol{B}_0$ configuration. All *Lagrangian* functions, $\boldsymbol{\Phi} = \hat{\boldsymbol{\Phi}}\left(\boldsymbol{X},t\right)$, depend on the shape parameters β_s through the variable $\boldsymbol{X}$.

- the *spatial* configuration: $\boldsymbol{B}_t$ at time t.
  This represents the state of the body after an elapsed time t. The points in this configurations will be denoted by $\boldsymbol{x}$ and the motion of the body is described with respect to the material configuration by:

$$\boldsymbol{x} = \hat{\boldsymbol{x}}\left(\boldsymbol{X},t\right) \tag{2}$$

  and with respect to the reference configuration by:

$$\boldsymbol{x} = \hat{\boldsymbol{x}}\left(\hat{\boldsymbol{X}}\left(\boldsymbol{Y};\beta_s\right),t\right) = \tilde{\boldsymbol{x}}\left(\boldsymbol{Y},t;\beta_s\right) \tag{3}$$

  All *Eulerian* functions, $\boldsymbol{\Phi} = \hat{\boldsymbol{\Phi}}\left(\boldsymbol{x},t\right)$, depend on the shape parameters β_s through the variables $\boldsymbol{x}$ and $\boldsymbol{X}$.

3 THE SHAPE DERIVATIVES

The objective of this work is to optimize the design parameters β_s in order to obtain a desirable product after the deformation process. In the final product, the desirable qualities may be a required final shape, homogeneous material properties, or a desirable residual stress/plastic strain distribution. Solution to these preform problems can be generally achieved by minimizing with respect to β_s certain cost functionals based on the geometry, stress or state variable fields in the final product. Therefore, one needs to evaluate the derivatives of these variable fields in the direction of the design parameters.

We define the shape derivative of a variable field (Sokolowski and Zolesio 1992) as below:

> The *shape derivative*, $\overset{\circ}{\boldsymbol{\Phi}}$ of a scalar, vector or tensor valued function $\boldsymbol{\Phi}$ is the total Gateaux derivative of $\boldsymbol{\Phi}$ in the direction of $\Delta\beta_s$ computed at β_s:

$$\overset{\circ}{\boldsymbol{\Phi}}\left(\beta_s,\Delta\beta_s\right) = \left.\frac{d}{d\lambda}\boldsymbol{\Phi}\left(\beta_s+\lambda\Delta\beta_s\right)\right|_{\lambda=0}$$

The shape derivative can be understood as the difference between two fields representing the same physical quantity

$\boldsymbol{\Phi}$, created by two different processes with slightly different parameters: β_s and $\beta_s + \Delta\beta_s$, i.e.:

$$\overset{\circ}{\boldsymbol{\Phi}} (\beta_s, \Delta\beta_s) = \boldsymbol{\Phi}(\beta_s + \Delta\beta_s) - \boldsymbol{\Phi}(\beta_s) + \mathcal{O}(||\Delta\beta_s||^2)$$

It should be noted that the comparison of the fields $\boldsymbol{\Phi}(\Delta\beta_s)$ and $\boldsymbol{\Phi}(\beta_s + \Delta\beta_s)$ is made at points of the reference configuration $\boldsymbol{B}_R$. The shape derivatives provide a measure of the change in a variable field due to a small change in the initial shape of the body.

4 THE DIRECT PROBLEM

The direct problem involves finding the time history of the deformation and the material state of a body deforming under the action of known external forces acting on it. The constitutive behavior follows the hyperelastic viscoplastic model developed by Brown et al. 1989. The computational aspects of the direct problem have been dealt with in Weber and Anand 1990 and Badrinarayanan and Zabaras 1993. Here, a brief review of the direct problem is presented to provide the necessary background for the sensitivity analysis.

The motion of the body was represented by a smooth mapping in equation (2). For this motion, the deformation gradient $\boldsymbol{F}$ defined over the material configuration is expressed as,

$$\boldsymbol{F} = \nabla\ \hat{\boldsymbol{x}}(\boldsymbol{X}, t) \tag{4}$$

This deformation gradient is decomposed as follows:

$$\boldsymbol{F} = \boldsymbol{F}^e\ \bar{\boldsymbol{F}}^p, \qquad \det \boldsymbol{F}^e > 0 \tag{5}$$

where, $\boldsymbol{F}^e$ is the elastic deformation gradient and $\bar{\boldsymbol{F}}^p$, the plastic deformation gradient, with $\det \bar{\boldsymbol{F}}^p = 1$. The elastic deformation gradient $\boldsymbol{F}^e$ has a unique polar decomposition given by:

$$\boldsymbol{F}^e = \boldsymbol{R}^e\ \boldsymbol{U}^e \tag{6}$$

The equilibrium equations can be expressed in the material configuration as:

$$\nabla \boldsymbol{\cdot} \boldsymbol{P} + \boldsymbol{f} = \boldsymbol{0},\ \forall\ \ \boldsymbol{X} \in\ \boldsymbol{B}_0 \quad \text{and} \quad \forall\ \ t \in\ [0, t_f] \tag{7}$$

where $\boldsymbol{P}(\boldsymbol{X}, t)$ is the Piola Kirchoff stress measure (or the nominal stress) and $\boldsymbol{f}$ the body force in the material configuration:

$$\begin{aligned} \boldsymbol{P}(\boldsymbol{X}, t) &= \det \boldsymbol{F}\ \boldsymbol{T}\ \boldsymbol{F}^{-T} \\ \boldsymbol{f}(\boldsymbol{X}, t) &= \det \boldsymbol{F}\ \boldsymbol{b} \end{aligned} \tag{8}$$

Here, $\boldsymbol{T}$ is the Cauchy stress tensor field determined by the equilibrium equations and $\boldsymbol{b}$ the *known* body force field.

A linear hyperelastic law relating the rotation neutralized Kirchoff stress $\bar{\boldsymbol{T}}$ and the logarithmic strain is assumed as:

$$\bar{\boldsymbol{T}} = \boldsymbol{\mathcal{L}}^e\ \left[\bar{\boldsymbol{E}}^e\right] \tag{9}$$

where,

$$\bar{\boldsymbol{T}} = (\det \boldsymbol{U}^e)\ \ (\boldsymbol{R}^e)^T\ \ \boldsymbol{T}\ \boldsymbol{R}^e \tag{10}$$

and

$$\bar{\boldsymbol{E}}^e = \ln(\boldsymbol{U}^e) \tag{11}$$

with $\boldsymbol{\mathcal{L}}^e$ the isotropic elastic moduli.

The evolution of the plastic deformation gradient can be expressed as

$$\frac{d}{dt}\left(\bar{\boldsymbol{F}}^p\right)\left(\bar{\boldsymbol{F}}^p\right)^{-1} = \bar{\boldsymbol{D}}^p \tag{12}$$

where the rate of plastic deformation gradient $\bar{\boldsymbol{D}}^p$ is written as:

$$\bar{\boldsymbol{D}}^p = \dot{\tilde{\epsilon}}^p\ \frac{3}{2}\frac{\bar{\boldsymbol{T}}'}{\tilde{\sigma}}$$

with the plastic strain rate $\dot{\tilde{\epsilon}}^p$ defined as a scalar function:

$$\dot{\tilde{\epsilon}}^p = f(\tilde{\sigma}, s) \tag{13}$$

and the equivalent stress, $\tilde{\sigma}$, given as:

$$\tilde{\sigma} = \sqrt{\frac{3}{2}\ \bar{\boldsymbol{T}}' \boldsymbol{\cdot} \bar{\boldsymbol{T}}'} \tag{14}$$

Also, $\bar{\boldsymbol{T}}'$ is the deviatoric part of $\bar{\boldsymbol{T}}$ given by

$$\bar{\boldsymbol{T}}' = \bar{\boldsymbol{T}} - \frac{1}{3}\ \text{tr}(\bar{\boldsymbol{T}})\ \boldsymbol{I} \tag{15}$$

Now, the evolution of the plastic deformation gradient can be re-written as,

$$\frac{d}{dt}\left(\bar{\boldsymbol{F}}^p\right)\left(\bar{\boldsymbol{F}}^p\right)^{-1} = \frac{3}{2}\ \frac{f(\tilde{\sigma}, s)}{\tilde{\sigma}}\ \ \bar{\boldsymbol{T}}' \tag{16}$$

Finally, the evolution of the scalar variable s (internal resistance to plastic deformation) is given as

$$\frac{d}{dt}(s) = g(\tilde{\sigma}, s) \tag{17}$$

In conclusion, for the above model, a deformed configuration of the body can be completely characterized by:

- the deformation gradient $\boldsymbol{F}$
- the triad of variables $\boldsymbol{V} = \left(\boldsymbol{T}, \bar{\boldsymbol{F}}^p, s\right)$

The functions $f(\tilde{\sigma}, s)$ and $g(\tilde{\sigma}, s)$ are experimentally determined for a particular material. Equations (2) and (4) – (17), together with the initial conditions on the scalar state variable s and the Cauchy stress $\boldsymbol{T}$, and the boundary conditions on the motion of the body, completely determine the direct problem. In a forming process, the boundary conditions are determined by the rigidity of the die, the die – workpiece interface friction conditions and the applied traction or displacement boundary conditions on the workpiece.

In an updated Lagrangian FEM formulation, one considers a sequence of time incremental problems from time

t_n to $t_{n+1}, n = 0, 1, 2, \ldots$. The configuration of the body at time t_n is used as the reference configuration for the incremental process. Two sub-problems are defined: first the *kinematic incremental problem*, where given the triad $\boldsymbol{V}$ at the beginning and the end of the time step and the external forces acting on the body, one calculates the incremental deformation gradient; and second, the *constitutive problem* where one evaluates the triad $\boldsymbol{V}$ at the end of the step given the configuration of the body at the beginning and the end of the time step and $\boldsymbol{V}$ at the beginning of the step. The kinematic problem requires full linearization of the principle of virtual work and the calculation of the consistent material linearized moduli. The constitutive problem is handled with the radial return mapping. The kinematic incremental problem and the constitutive problem are coupled and must be solved iteratively within a time step.

5 SHAPE SENSITIVITY ANALYSIS

In the analysis performed below, we assume that the material state and deformation history for each parameter β_s (i.e. for each preform shape) are known from the solution of the corresponding direct problem. The dependence of the shape sensitivity fields on the material state history and deformation will not be shown explicitly.

Similar to the direct problem, the sensitivity problem is subdivided into two problems: the constitutive and the kinematic. In the *constitutive problem*, it is assumed that the sensitivity of the triad $\overset{\circ}{\boldsymbol{V}}_n$ is known at the beginning of a time step $t = t_n$. The objective is to determine the dependence of $\overset{\circ}{\boldsymbol{V}}_{n+1}$ on the sensitivity of the total deformation gradient $\overset{\circ}{\boldsymbol{F}}_{n+1}$. In the *kinematic problem*, using a principle of virtual work like equation for the sensitivity fields, one has to determine the sensitivity of the deformation gradient $\overset{\circ}{\boldsymbol{F}}_{n+1}$ at the end of the time step, knowing $\overset{\circ}{\boldsymbol{V}}_n$, the linear relationship between $\overset{\circ}{\boldsymbol{V}}_{n+1}$ and $\overset{\circ}{\boldsymbol{F}}_{n+1}$, and by applying appropriate boundary conditions for $\overset{\circ}{\boldsymbol{F}}_{n+1}$. Once $\overset{\circ}{\boldsymbol{F}}_{n+1}$ is calculated from the kinematic problem, the linear relationship derived in the constitutive problem can be used to obtain the sensitivity of the triad $\overset{\circ}{\boldsymbol{V}}_{n+1}$. The two problems are linearly coupled and together provide a *single linear* problem for the calculation of the sensitivities of both the deformation and the material state.

5.1 *Shape derivatives of constitutive equations*

The mathematical analysis for the derivation of the shape derivatives of the constitutive equations is similar to that developed for process derivatives as presented in Badrinarayanan and Zabaras 1995. Here, we provide only the final results in a concise form.

The shape derivative of the Cauchy Stress $\boldsymbol{T}$ is expressed as:

$$\overset{\circ}{\boldsymbol{T}} = (\det \boldsymbol{U}^e)^{-1}\, \boldsymbol{R}^e\, \overset{\circ}{\bar{\boldsymbol{T}}}\, (\boldsymbol{R}^e)^T - \mathrm{tr}\left(\overset{\circ}{\bar{\boldsymbol{E}}}{}^e\right) \boldsymbol{T} + \left(\overset{\circ}{\boldsymbol{R}}{}^e\, (\boldsymbol{R}^e)^T\, \boldsymbol{T} - \boldsymbol{T}\, \overset{\circ}{\boldsymbol{R}}{}^e\, (\boldsymbol{R}^e)^T\right) \tag{18}$$

where

$$\overset{\circ}{\boldsymbol{R}}{}^e\, (\boldsymbol{R}^e)^T = \overset{\circ}{\boldsymbol{F}}{}^e\, (\boldsymbol{F}^e)^{-1} - \boldsymbol{R}^e\, \mathrm{sym}\left((\boldsymbol{U}^e)^{-1}\, \mathrm{sym}\left((\boldsymbol{F}^e)^T\, \overset{\circ}{\boldsymbol{F}}{}^e\right)\right)(\boldsymbol{U}^e)^{-1}\, (\boldsymbol{R}^e)^T \tag{19}$$

$$\overset{\circ}{\boldsymbol{U}}{}^e = \mathrm{sym}\left((\boldsymbol{U}^e)^{-1}\, \mathrm{sym}\left((\boldsymbol{F}^e)^T\, \overset{\circ}{\boldsymbol{F}}{}^e\right)\right) \tag{20}$$

$$\overset{\circ}{\bar{\boldsymbol{E}}}{}^e = 4\, (\boldsymbol{U}^e + \boldsymbol{I})^{-1}\, \overset{\circ}{\boldsymbol{U}}{}^e\, (\boldsymbol{U}^e + \boldsymbol{I})^{-1} \tag{21}$$

$$\overset{\circ}{\bar{\boldsymbol{T}}} = \boldsymbol{\mathcal{L}}^e\left[\overset{\circ}{\bar{\boldsymbol{E}}}{}^e\right] \tag{22}$$

$$\overset{\circ}{\bar{\boldsymbol{T}}}{}' = \overset{\circ}{\bar{\boldsymbol{T}}} - \frac{1}{3}\mathrm{tr}\left(\overset{\circ}{\bar{\boldsymbol{T}}}\right)\, \boldsymbol{I} \tag{23}$$

and

$$\overset{\circ}{\tilde{\sigma}} = \frac{3}{2}\frac{\bar{\boldsymbol{T}}' \cdot \overset{\circ}{\bar{\boldsymbol{T}}}{}'}{\tilde{\sigma}} \tag{24}$$

The evolution equation for the direct problem can be directly differentiated to obtain the evolution equations for the sensitivity fields. Employing Euler backward integration, these evolution equations can be integrated to obtain:

$$\overset{\circ}{s}_{n+1} = \overset{\circ}{s}_n\, \exp(g_s \Delta t) + \frac{g_{\tilde{\sigma}}}{g_s}\, \overset{\circ}{\tilde{\sigma}}_{n+1}\, [\exp(g_s \Delta t) - 1] \tag{25}$$

and

$$\overset{\circ}{\bar{\boldsymbol{F}}}{}^p{}_{n+1} = \exp\left(\Delta t\, \bar{\boldsymbol{D}}^p_{n+1}\right)\, \overset{\circ}{\bar{\boldsymbol{F}}}{}^p{}_n + \left[\exp\left(\Delta t\, \bar{\boldsymbol{D}}^p_{n+1}\right) - \boldsymbol{I}\right]\left(\bar{\boldsymbol{D}}^p_{n+1}\right)^{-1}\, \overset{\circ}{\bar{\boldsymbol{D}}}{}^p{}_{n+1}\, \bar{\boldsymbol{F}}^p_{n+1} \tag{26}$$

where

$$\exp\left(\Delta t\, \bar{\boldsymbol{D}}^p_{n+1}\right) = \bar{\boldsymbol{F}}^p_{n+1}\left(\bar{\boldsymbol{F}}^p_n\right)^{-1} \tag{27}$$

From the multiplicative decomposition we obtain,

$$\overset{\circ}{\boldsymbol{F}}_{n+1} = \overset{\circ}{\boldsymbol{F}}{}^e{}_{n+1}\, \bar{\boldsymbol{F}}^p_{n+1} + \boldsymbol{F}^e_{n+1}\, \overset{\circ}{\bar{\boldsymbol{F}}}{}^p{}_{n+1} \tag{28}$$

This equation can now be solved to express $\overset{\circ}{\boldsymbol{F}}{}^e{}_{n+1}$ as a linear function of $\overset{\circ}{\boldsymbol{F}}_{n+1}$. This in turn will imply that $\overset{\circ}{\boldsymbol{T}}_{n+1}$ can be written as a linear function of $\overset{\circ}{\boldsymbol{F}}_{n+1}$. For further discussion on many of the issues involved in the above derivation, refer to Badrinarayanan and Zabaras 1995.

5.2 *Shape derivative of the equilibrium equations*

We define the *reference* gradient of every material point $\boldsymbol{X}$ in the configuration $\boldsymbol{B}_0$ as below:

$$\boldsymbol{F}_R(\boldsymbol{Y};\beta_s) = \nabla_Y \boldsymbol{X} = \frac{\partial \boldsymbol{X}}{\partial \boldsymbol{Y}} \tag{29}$$

We further define $\boldsymbol{L}_R$ as:

$$\boldsymbol{L}_R = \overset{\circ}{\boldsymbol{F}}_R \;\; \boldsymbol{F}_R^{-1} \tag{30}$$

We start from the local form of the equilibrium equation (7) on the material configuration $\boldsymbol{B}_0$, and determine the shape derivative of the equilibrium equation. In doing so, it has to be noted that all the spatial derivatives are evaluated with respect to the configuration $\boldsymbol{B}_0$. In the sequel, all spatial derivatives we mention are assumed to be evaluated with respect to $\boldsymbol{B}_0$.

It can be shown that

$$\overset{\circ}{(\nabla \boldsymbol{\cdot} \boldsymbol{P})} = \nabla \boldsymbol{\cdot} \; \overset{\circ}{\boldsymbol{P}} + \nabla \boldsymbol{\cdot} \left(\boldsymbol{P}\boldsymbol{L}_R^T\right) - \boldsymbol{P}\left[\nabla \boldsymbol{\cdot} \boldsymbol{L}_R^T\right] \tag{31}$$

Thus, the shape derivative of the equilibrium equation becomes:

$$\nabla \boldsymbol{\cdot} \left(\overset{\circ}{\boldsymbol{P}} + \boldsymbol{P}\boldsymbol{L}_R^T\right) - \boldsymbol{P}\left[\nabla \boldsymbol{\cdot} \boldsymbol{L}_R^T\right] + \overset{\circ}{\boldsymbol{f}} = \boldsymbol{0}$$

$$\forall \;\; \boldsymbol{X} \in \;\; \boldsymbol{B}_0 \text{ and } \forall \;\; t \in \; [0, t_f] \tag{32}$$

where, $\overset{\circ}{\boldsymbol{P}}$ is obtained as

$$\overset{\circ}{\boldsymbol{P}} = \det \boldsymbol{F}\left[\operatorname{tr}\left(\overset{\circ}{\boldsymbol{F}}\;\boldsymbol{F}^{-1}\right)\boldsymbol{T} + \overset{\circ}{\boldsymbol{T}} - \boldsymbol{T}\left(\overset{\circ}{\boldsymbol{F}}\;\boldsymbol{F}^{-1}\right)^T\right]\boldsymbol{F}^{-T} \tag{33}$$

The weak form for the above equation (32) is given as:

$$\int_{\boldsymbol{B}_0} \overset{\circ}{\boldsymbol{P}} \boldsymbol{\cdot} \frac{\partial \tilde{\boldsymbol{u}}}{\partial \boldsymbol{X}} \, dV_0 -$$

$$\int_{\partial \boldsymbol{B}_{n+1}} \left\{\left(\overset{\circ}{\boldsymbol{F}}\;\boldsymbol{F}^{-1}\right) \boldsymbol{\cdot} \left(\boldsymbol{I} - \boldsymbol{n}\otimes\boldsymbol{n}\right)\right\} \hat{\boldsymbol{t}} \boldsymbol{\cdot} \tilde{\boldsymbol{u}} \; dA_{n+1} =$$

$$\int_{\boldsymbol{B}_0} \left(\boldsymbol{P}\left[\nabla \boldsymbol{\cdot} \boldsymbol{L}_R^T\right]\right) \boldsymbol{\cdot} \tilde{\boldsymbol{u}} \; dV_0 + \int_{\boldsymbol{B}_0} \left(\boldsymbol{P}\boldsymbol{L}_R^T\right) \boldsymbol{\cdot} \frac{\partial \tilde{\boldsymbol{u}}}{\partial \boldsymbol{X}} \, dV_0 +$$

$$\int_{\partial \boldsymbol{B}_{n+1}} \left(\overset{\circ}{\hat{\boldsymbol{t}}} - \left(\boldsymbol{F}\boldsymbol{L}_R\boldsymbol{F}^{-1} \boldsymbol{\cdot} \left(\boldsymbol{n}\otimes\boldsymbol{n}\right)\right)\hat{\boldsymbol{t}}\right) \boldsymbol{\cdot} \tilde{\boldsymbol{u}} \; dA_{n+1} \tag{34}$$

for admissible values of $\tilde{\boldsymbol{u}}$.

5.3 *The force terms*

Foe a finite element implementation of the weak form of the sensitivity equilibrium equations, one must evaluate the corresponding stiffness matrix and force vector. Here, we deal in some detail with the calculation of the force terms.

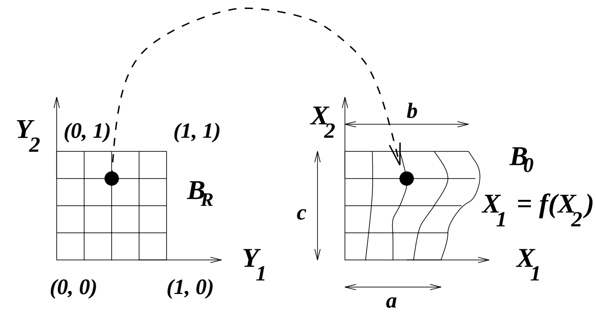

Figure 2: A mapping from the reference configuration to the material configuration

In order to evaluate the force terms, we need to calculate the quantities $\boldsymbol{L}_R$ and $\overset{\circ}{\hat{\boldsymbol{t}}}$. $\boldsymbol{L}_R$ depends on the variation in the design parameter β_s. In two dimensions, the reference configuration $\boldsymbol{B}_R$ is taken to be a unit square. For demonstration of ideas, let us consider the case (refer to figure (2)) where three of the boundary segments of $\boldsymbol{B}_0$ are flat, while the right hand side boundary segment is represented by the equation $\boldsymbol{X}_1 = f(\boldsymbol{X}_2)$. Here, f is a function approximated as follows:

$$f(\boldsymbol{X}_2) = \sum_{i=1}^{n} \beta_i \phi_i(\boldsymbol{X}_2) \tag{35}$$

with $f(0) = a$ and $f(c) = b$. Also, $(\phi_1, \phi_2, \ldots, \phi_n)$ are appropriately selected basis shape functions and $(\beta_1, \beta_2, \ldots, \beta_n)$ a set of n scalar parameters. Applying a linear transfinite mapping for this boundary representation (George 1991), one can introduce a mapping $\hat{\boldsymbol{X}}(\boldsymbol{Y};\beta_s)$ as below:

$$(\boldsymbol{X}_1, \boldsymbol{X}_2) = (\boldsymbol{Y}_1 f(c\boldsymbol{Y}_2), c\boldsymbol{Y}_2) \tag{36}$$

Therefore, for this case,

$$\boldsymbol{F}_R = \begin{bmatrix} f(c\boldsymbol{Y}_2) & c\boldsymbol{Y}_1 f'(c\boldsymbol{Y}_2) \\ 0 & c \end{bmatrix} \tag{37}$$

where f' denotes the derivative of f. If we perturb a parameter, say, β_k by $\Delta\beta_k$ while keeping all the other parameters constant, we can obtain $\overset{\circ}{\boldsymbol{F}}_R$ as

$$\overset{\circ}{\boldsymbol{F}}_R = \Delta\beta_k \begin{bmatrix} \phi_k(c\boldsymbol{Y}_2) & c\boldsymbol{Y}_1 \phi_k'(c\boldsymbol{Y}_2) \\ 0 & 0 \end{bmatrix} \tag{38}$$

From $\boldsymbol{F}_R$ and $\overset{\circ}{\boldsymbol{F}}_R$, one can calculate $\boldsymbol{L}_R$. Solving the weak shape sensitivity problem with this $\boldsymbol{L}_R$ induced by a change of $\Delta\beta_k$, one can evaluate at the direct solution corresponding to $(\beta_1, \beta_2, \ldots, \beta_n)$, the gradient of the objective function in the direction of the kth design variable (Badrinarayanan and Zabaras 1995).

Calculation of $\overset{\circ}{\hat{\boldsymbol{t}}}$ depends on the type of traction forces applied on the boundary. If the dependence of the $\hat{\boldsymbol{t}}$ on

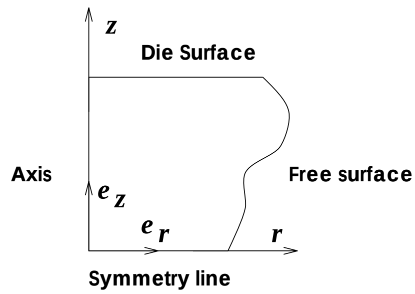

Figure 3: Preform shape for the upset forging

the geometry is well known, the shape derivative of $\hat{\boldsymbol{t}}$ can be easily evaluated. A method similar to that developed in Badrinarayanan and Zabaras 1995 can be applied when the traction condition is indirectly specified as in the case of sliding friction.

6 APPLICATION

We consider a preform design problem in open die forging of a cylindrical Aluminum workpiece, where we want to achieve a final product without barreling. The material constants are taken from Brown et. al. 1989. The die-workpiece interface is modelled with sticking friction. The cylinder is assumed to be axially symmetric and also symmetric about a plane parallel to the flat die surface. The geometry of the workpiece is shown in figure (3). The free surface is modelled using 3 pieces of cubic splines and 7 independent parameters β_i. Let the free surface of the deformed body in the final configuration be denoted by Γ_f. Then, the optimization problem can be written as

$$\min_{\beta_i} \int_{\Gamma_f} (\boldsymbol{x} \bullet \boldsymbol{e}_r - r_0)^2 \, dl \tag{39}$$

Subject to the constraint

$$\int_{\boldsymbol{B}_{0(\beta_i)}} dV = V_0 \tag{40}$$

where $\boldsymbol{e}_r$ is the unit radial vector, V_0, the volume of the cylinder and r_0 the radius of the cylinder that would have resulted while upsetting a cylindrical piece of volume V_0 under frictionless conditions. In order to obtain the optimal solution for this problem, we need to evaluate the gradients of $\boldsymbol{x} \in \Gamma_f$ with respect to the parameters β_i. We employ the sensitivity analysis developed in the previous sections to obtain the shape sensitivities and from them we compute the gradient of the objective function. The calculated sensitivities are within 1% compared to the finite difference solutions obtained using the direct results corresponding to two nearby preforms.

The optimization is performed using a modified BFGS algorithm. The solution is assumed to converge when $(||\Delta\beta_s||)/||\beta_s|| < 1\%$.

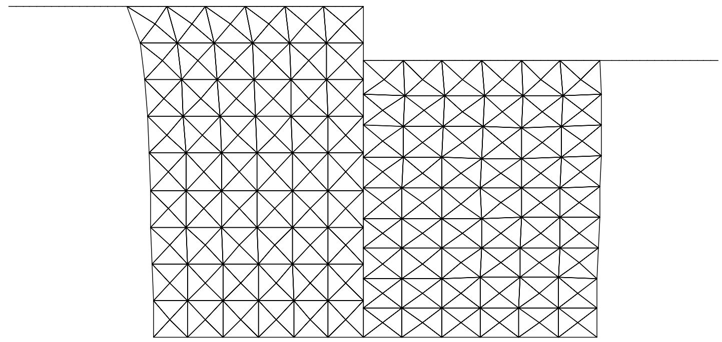

Figure 4: Undeformed and deformed configurations of the optimal preform shape for a 16.67% height reduction

We start from the initial design of a flat free surface which results in barreling in the final product. A deformation corresponding to 16.67% reduction in height is imposed and the preform shape that leads to a product with no barreling is obtained. The result is shown in figure (4). A similar problem was solved in Fourment and Chenot 1994 with a coarser mesh and for a simpler material model. The optimal preform shape reported there follows a similar trend to that of figure (4).

Let us now consider a substantial deformation (44.44% height reduction) which results in a fold over of the workpiece. The finite element mesh is reasonably fine in the region where fold over occurs. An optimal preform shape for this height reduction is obtained using the same optimization algorithm. The initial preform shape is shown in figure (5) and the optimal preform in figure (6). The preform shape obtained for this height reduction is considerably different from that of figure (4), especially in the regions where fold over occurs. With an even finer mesh near the fold over region and a better representation of the free surface, one, at the expense of a higher computational cost, could obtain in a fine detail the preform shape that leads to a perfectly flat free surface in the final product. Obviously, even in that case, the material properties will not be uniformly distributed in the final product.

7 CONCLUSIONS

A shape sensitivity analysis method has been developed for large deformation of hyperelastic viscoplastic solids that can be applied to preform design problems in metal forming. A principle of virtual work like equation is developed for the shape sensitivity fields. The calculated sensitivity fields are very accurate and satisfactory results were obtained while designing preform shapes for open die forging.

8 ACKNOWLEDGEMENTS

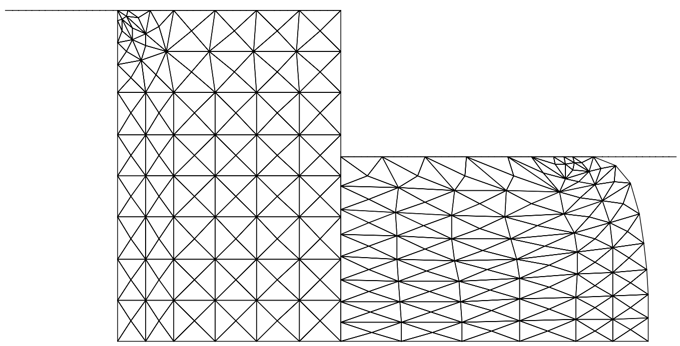

Figure 5: Undeformed and deformed configurations of the initial preform shape for a 44.44% height reduction

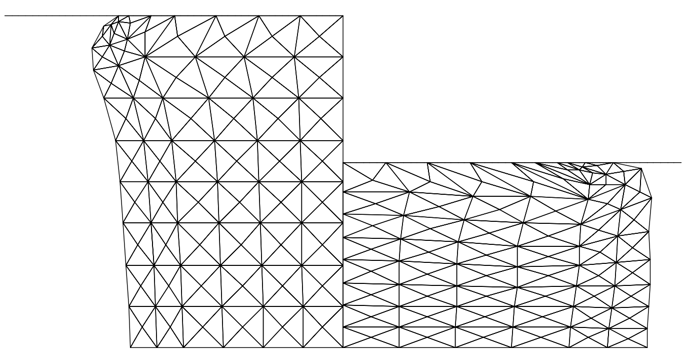

Figure 6: Undeformed and deformed configurations of the optimal preform shape for a 44.44% height reduction

This work was funded by NSF grant DDM-9157189 to Cornell University. The computing was supported from the Cornell Theory Center.

REFERENCES

Badrinarayanan, S. and N. Zabaras 1993. A Two- Dimensional FEM Code for the Analysis of Large Deformations of Hyperelastic-Viscoplastic Solids, *Technical Report MM-93-05, Materials Processing Program, Sibley School of Mechanical and Aerospace Engineering, Cornell University.*

Badrinarayanan, S. and N. Zabaras 1995. A Sensitivity Analysis for the Optimal Design of Metal Forming Processes. Accepted in *Comp. Meth. Appl. Mech. Eng.*

Brown, S.B., K.H.Kim and L. Anand 1989. An Internal Variable Constitutive Model for Hot Working of Metals. *Int. J. Plasticity* 5:95-130.

Fourment, L. and J.L. Chenot 1994. The Inverse Problem of Design in Forging. *Inverse Problems in Engineering Mechanics, (edts. H.D. Bui et al.)* 21-28. Balkema, Rotterdam.

George, P.L. 1991. *Automatic Mesh Generation: Application to Finite Element Methods.* John Wiley and Sons, New York.

Kobayashi, S., S. Oh and T. Altan 1989. *Metal Forming and the Finite-Element Method.* Oxford University Press, New York.

Lee, T.H. and J.S. Arora 1993. Shape Design Sensitivity Analysis of Viscoplastic Structures. *Comp. Meth. Appl. Mech. Eng.* 108:237-259.

Fletcher, R. 1987. *Practical Methods of Optimization.* John Wiley and Sons, New York.

Sokolowski, J. and J.P. Zolesio 1992. *Introduction to Shape Optimization - Shape Sensitivity Analysis.* Springer-Verlag, New York.

Tortorelli, D.A. and P. Michaleris 1994. Design Sensitivity Analysis: Overview and Review. *Inv. Prob. in Eng.* 1:71-105.

Vidal, C.A. and R.B. Haber 1993. Design Sensitivity Analysis for Rate-Independent Elastoplasticity. *Comp. Meth. Appl. Mech. Eng.* 107:393-431.

Weber, G. and L. Anand 1990. Finite deformation constitutive equations and a time integration procedure for isotropic, hyperelastic-viscoplastic solids. *Comp. Meth. App. Mech. Eng.* 79:173-202.

Zabaras, N. and S. Badrinarayanan 1993. Inverse Problems and Techniques in Metal Forming Processes. *Inverse Problems in Engineering: Theory and Practice (edts. N.Zabaras et al.)* 65-76. ASME, New York, N.Y.